Standardizing Characterization of Electromagnetic Water Content Sensors: Part II. Evaluation of Seven Sensing Systems

J. M. Blonquist Jr.*

S. B. Jones

D. A. Robinson

Dept. of Plants, Soils and Biometeorology, Utah State University,

4820 Old Main Hill, Logan, UT, USA 84322-4820

*Corresponding Author

Email: jmarkb@cc.usu.edu

Characterization and Calibration of Seven Electromagnetic Water Content Sensors: Part II. Evaluation of Seven Sensing Systems

ABSTRACT

Transmission line-type electromagnetic (EM) methods for estimating soil volumetric water content (q_v) have advanced significantly in recent years with many sensing systems available. In order to estimate q_v, EM systems make use of the dependence of soil dielectric permittivity on q_v. However, a standard method for characterizing and comparing EM system measurement capability has not been established. Our objective was to evaluate the permittivity measurement ability of seven different EM sensing systems using readily available media. Sensing system outputs were converted to real permittivity (e') values and compared to reference e' values in lossless and lossy dielectric liquids under four different test conditions; non-relaxing and non-conducting (NR-NC), relaxing and non-conducting (R-NC), non-relaxing and electrically conducting (NR-C) and temperature variation in NR-NC. The higher frequency broadband sensing systems, consisting of two time domain reflectometry (TDR) systems and one time domain transmissometry (TDT) system, deviated from a network analyzer by less than ± 2.94 e' units across a e' range of 12.7 to 78.5 in NR-NC media. Two lower frequency impedance sensing systems deviated from the network analyzer by less than ± 3.94 e' units across a e' range of 12.7 to 36.5 in the same media. Measurement of e' using higher frequency broadband sensing systems was impacted more by bulk electrical conductivity (s_b) and temperature (T) than by

dielectric relaxation. Imaginary permittivity values (due only to relaxation, ε''_{rel}) of up to 14.5 in R-NC media resulted in ε' errors of ± 0.511, whereas σ_b values ranging from 0 to 2 dS m^{-1} in NR-C media resulted in ε' errors of ± 2.69 and T values ranging from 5 to 40 °C resulted in ε' errors of ± 4.89. Determination of ε' using lower frequency sensing systems; including one transmission line oscillator, two impedance probes and one capacitance probe; was impacted more by σ_b than by T and ε''_{rel}. For the lower frequency sensors (and the same ranges of σ_b, T and ε''_{rel}), σ_b resulted in ε' errors of ± 111, T resulted in ε' errors of ± 6.59 and ε''_{rel} resulted in ε' errors of ± 3.28. The effects of ε''_{rel}, σ_b and T on permittivity measurement accuracy is to a large extent dependent on measurement frequency; with higher frequency broadband sensing systems generally yielding better measurements.

INDEX TERMS: TDR, EM sensors, permittivity, soil water content

INTRODUCTION

It has been established that for many coarse-textured mineral soils there is a strong relationship between the dielectric permittivity (e; all permittivity values discussed herein are relative to free space) determined with transmission line-type electromagnetic (EM) sensors and soil volumetric water content (q_v) (Topp et al., 1980; Malicki et al., 1996). This is due to the strong contrast between the permittivity of water ($e \sim 80$), mineral soil solids ($e \sim 2\text{-}9$) and air ($e \sim 1$). Two-step (i.e. relation of measured property to e and e to q_v) and direct calibrations (i.e. relation of measured property to q_v) are used in estimating q_v from EM signal measurements (e.g. travel time, impedance, capacitor charge time, oscillation frequency, frequency shift). For accurate q_v estimations, sensing systems must make accurate EM signal property measurements that can be accurately related to q_v. Fellner-Felldeg (1969) demonstrated that transmission line methods, specifically time domain reflectometry (TDR), could be employed to measure e of liquids. Topp et al. (1980) extended TDR measurements to soils and empirically related TDR-estimated e to q_v. Estimates of q_v using TDR have been shown to be quite accurate, with the error reported at less than $\pm$ 0.02 m^3 m^{-3} in many coarse-textured mineral soils (Topp et al., 1980; Topp et al., 1982; Hook and Livingston, 1995).

Since Topp et al's. (1980) seminal work in soils, much effort has focused on improving the $e - q_v$ relationship (Roth et al., 1990; Dirksen and Dasberg, 1993; Jacobsen and Schjonning, 1993; Whalley, 1993; Heimovaara et al., 1994; Malicki et al., 1996; Friedman, 1998; Ponizovsky et al., 1999). Work has also focused on evaluating EM sensing system performance in a number

of soils at varying q_v ranges (Evett et al., 2002; Leib et al., 2003; Walker et al., 2004). However, EM signal measurements are sensitive to factors (e.g. dielectric relaxation, electrical conductivity, temperature) beyond q_v, and signal measurements must be accurate before relation to q_v. For this reason Jones et al. (this issue) proposed a standard method employing measurements in liquids to characterize and compare EM sensing system measurements. Liquids provide homogeneous backgrounds as opposed to soils, which may enhance unwanted noise and uncertainty in the measurements owing to secondary factors (Jones and Or, 2002; 2003). Liquids also eliminate contact problems between the medium and probe, which may occur in soils. Our objective was to demonstrate and test the proposed method of Jones et al. (this issue) for characterizing and comparing EM signal measurement accuracy and range by applying it to seven different q_v sensing systems.

MATERIALS AND METHODS

Sensing Systems Considered

The sensing systems considered are a TDR cable tester (Tektronix Inc., Beaverton, OR; 1502B Metallic Cable Tester) connected to a custom 3-rod probe with 0.15-m long, 3.20-mm diameter rods and 12.0-mm rod spacing; a second TDR instrument (Campbell Scientific Inc., Logan, UT; TDR100) connected to the same probe described above; a time domain transmissometry (TDT) system (Acclima Inc., Meridian, ID; Digital TDT Moisture Sensor); a transmission line oscillator (Campbell Scientific Inc., Logan, UT; CS616 Water Content

Reflectometer); an impedance probe (Stevens Water Monitoring Systems Inc., Beaverton, OR; Hydra Soil Moisture Probe); a second impedance probe (Dynamax Inc., Houston, TX; Theta Probe type ML2x) and a capacitance probe (Decagon Devices Inc., Pullman, WA; ECH$_2$O Probe model EC-20) (Table 1 and Figure 1).

The EM signal properties (i.e. travel time, period, impedance and charge time) measured by the sensing systems listed are directly related to the e of the medium in which they are embedded. The TDR and TDT sensing systems measure the travel time (t) of a broadband EM signal propagating along the probe and relate t to apparent permittivity (K_{TDR}), which subsequently relates to q_v. Calculation of K_{TDR} (= real permittivity (e') in lossless media) from t [s] measurements is accomplished according to:

$$K_{TDR} = \left(\frac{ct}{2L_e} \right)^2 . \qquad [1]$$

where c is the speed of light in vacuum ($3 \cdot 10^8$ m s^{-1}) and L_e is electrical length of the probe [m]. With TDR the signal is reflected at the end of the probe and the return signal is sampled. The factor 2 in the denominator of Eq. [1] accounts for the two-way (down and back) travel time of the signal. With TDT the signal travels the length of the probe once and the transmitted signal is sampled, thus the factor of 2 is omitted from Eq. [1]. It should be noted that both the Tektronix 1502B and the TDR100 account for the two-way travel time internally and waveforms are output to display one-way travel, thus the factor of 2 is omitted from Eq. [1] for the TDR systems as well.

The waveforms measured with the Tektronix TDR were captured and interpreted for travel time with WinTDR waveform analysis software (Or et al., 2003) on a personal computer. The waveforms measured with the TDR100 were interpreted for travel time with PCTDR software (available with purchase of TDR100) on a personal computer. The waveforms measured with the Acclima TDT were captured and interpreted for travel time measurement via custom firmware developed by Acclima and contained in the sensor head. Custom software developed by Acclima (available with purchase of Acclima system) was used to download data with the use of personal computer. Determination of the electrical length (L_e) and travel time of the signal in the sensor head for the 3-rod probe used with the Tektronix TDR and the TDR100, and the Acclima TDT, was conducted using measurements in air and de-ionized water according to the method described in Heimovaara (1993) and Robinson et al. (2003a). This procedure is outlined in Jones et al. (this issue); and t values measured with the described software and firmware were adjusted based on this procedure. Further detail concerning TDR systems and measurements is given in Robinson et al. (2003b) and further detail concerning the Acclima TDT system is given in Blonquist et al. (in review).

The CS616 Water Content Reflectometer is a transmission line oscillator and operates similar to TDR systems. Transmission line oscillators generate a voltage pulse inside the sensor head which propagates along the waveguide; with the arrival of the reflected pulse triggering the next pulse. The number of voltage pulse reflections over a certain time interval is recorded and a period [μs] that is inversely related to the number of reflections per second is output. The period is directly related to q_v via empirical calibration. Both a linear and a quadratic calibration

equation relating period to q_v are reported (Campbell Scientific, Inc., 2002-2003). It should be noted that the actual frequency of the EM signal pulse generated by the CS616 is not reported. A more detailed treatment of measurements with water content reflectometers is presented in Seyfried and Murdock (2001) in which they test and compare six CS615's in air, ethanol and four soils.

The Hydra Probe measures the ratio of reflected voltage to incident voltage of a 50 MHz signal, which is dependent on the impedance of the medium between the probe rods (Seyfried and Murdock, 2004). The Hydra Probe outputs four voltage values (V_1, V_2, V_3 and V_4) with V_1, V_2 and V_3 characterizing the capacitive and conductive properties of the medium and V_4 relating to temperature (Stevens Vitel, Inc., 1994). Custom software is employed to empirically calculate the real and imaginary parts of the permittivity and bulk electrical conductivity (s_b) from the output voltage values (Stevens Vitel, Inc., 1994). Estimation of q_v is accomplished via the software using an empirical calibration with real permittivity as the input value. A more detailed treatment of the Hydra Probe is presented in Seyfried and Murdock (2004) in which they test and compare three Hydra Probes in several fluids and four soils, and in the article by Seyfried et al. (this issue).

The Theta Probe measures the voltage amplitude difference (between the section of transmission line inside the sensor head and at the boundary between the sensor head and probe rods) of a 100 MHz signal, which is dependent on the impedance of the medium between the probe rods (Gaskin and Miller, 1996). The Theta Probe outputs a single voltage value that is

related to permittivity (K_{Theta}) via the following empirical relationship (Delta-T Devices Ltd., 1999):

$$\sqrt{K_{Theta}} = 1.07 + 6.40V - 6.40V^2 + 4.70V^3 \quad [2]$$

where V is volts. In order to estimate q_v with the Theta Probe, media specific calibration with estimated K_{Theta} values and known q_v values or use of established q_v prediction equations is required. A more detailed treatment of the Theta Probe is given in Gaskin and Miller (1996).

The ECH_2O Probe measures the charge time of a capacitor that uses the medium surrounding the probe as the dielectric material (Decagon Devices, Inc., 2002). The ECH_2O Probe outputs a single voltage value and directly relates this value to q_v via an empirical equation (Decagon Devices, Inc., 2002). It should be noted that the signal frequency at which the ECH_2O Probe operates is not reported. McMichael and Lascano (2003) tested and compared four ECH_2O Probes in water, two soils, and a potting medium.

For the CS616, Hydra Probe, Theta Probe and ECH_2O Probe; power was supplied, measurements were triggered, and period or voltage was recorded via connection to a Campbell Scientific CR23X data logger connected to a personal computer. Each sensing system's principle of operation, the equipment required for operation and cost comparisons of the systems (for single measurements and for simultaneous measurements with eight sensors) are summarized in Table 1.

Test Conditions

The measurements for the sensing system comparison were made under temperature controlled test conditions consisting of non-relaxing and non-conducting (NR-NC) media simulating non-saline, sandy soils; relaxing and non-conducting (R-NC) media simulating lower conductivity, clayey soils and non-relaxing and electrically conducting (NR-C) media simulating saline, sandy soils. Temperature effects in the NR-NC media were also characterized by varying the temperature. With each sensing system, we made three repetitions of each measurement at each point under the different test conditions, and the three repetitions were averaged to yield the measurement value for the given point.

The NR-NC media were made using fractions of de-ionized water mixed into 2-isopropoxyethanol with the permittivity extremes (e_s = 12.7 and e_s = 78.5; where e_s is the static real part of the permittivity) coming from pure 2-isopropoxyethanol and pure de-ionized water, respectively. The NR-C media were made from two mixtures (e_s = 40.0 and e_s = 78.5) of these same fluids and dissolving pre-determined amounts of sodium chloride (NaCl) into the solutions in order to create s_b ranging from 0.0 to 2.0 dS m^{-1}. The R-NC media consisted of glycerol (e_s = 46.5), Brasso® (e_s = 28.0), and 1-propanol (e_s = 22.8). We attempted to synthesize a relaxing and conducting (R-C) media; simulating high conductivity, clayey soils; by dissolving NaCl into the R-NC media, but were unable to reach s_b levels above approximately 0.3 dS m^{-1}. The test media, their associated properties and the temperature ranges measured in the media during the sensor measurements are summarized in Table 2. Further detail concerning test conditions and media is provided in Jones et al. (this issue).

Network analyzer (Hewlett Packard, Beaverton, OR, model 8752C network analyzer connected to model 85070B dielectric probe) measurements of the frequency dependent real (e') and imaginary parts (e'') of the permittivity of the described NR-NC and R-NC media were modeled with the Cole-Cole model (Hasted, 1973; Heimovaara, 1994; Eq. [9] in Jones et al., this issue). The Cole-Cole model was fit to the measured network analyzer data in order to provide media dependent parameter values and frequency dependent e' and e'' values for the range of operating frequencies of the sensing systems considered in the study. The network analyzer covers a frequency range of 300 kHz to 6 GHz, spanning the frequency ranges of the sensing systems. The network analyzer measurements and Cole-Cole model are described in further detail, and the models and parameter values are shown, in Jones et al. (this issue).

Frequency Determination, Response Modeling and Accuracy Assessment

Sensing system frequencies were determined in order to produce response models as explained in Jones et al. (this issue). The maximum passable frequency (f_{max}) was determined for the two TDRs connected to a 0.15-m long 3-rod probe (f_{max} is probe dependent) and the Acclima TDT in NR-NC media (ranging from e_s = 12.7 to e_s = 62.8) by matching K_{TDR} (= e' in NR-NC media) data from the sensing systems to frequency dependent e' from the network analyzer and averaging the results (Table 3). The f_{max} is the highest frequency component of the broadband signal and is the frequency at which measurements are made when tangent line fitting is used to determine permittivity from travel time. Greater detail concerning f_{max} determination for the two TDRs and TDT is found in Blonquist et al. (in review) and Jones et al. (this issue). Frequencies

for the Hydra Probe and Theta Probe (Table 3) are the reported frequencies (Stevens Vitel, Inc., 1994; Delta-T Devices Ltd., 1999; respectively). Frequencies for the CS616 and ECH$_2$O Probe (Table 3) were approximated from rise times of the incident voltage pulse of 2 ns (Campbell Scientific, personal communication) and 8 ns (Decagon Devices, personal communication), respectively, according to (Bogart et al., 2004):

$$f = \frac{0.35}{t_r} \quad [3]$$

where f is the frequency [Hz] of the signal corresponding to a measurement in air ($\sim f_{max}$ in NR-NC media) and t_r is rise time [s]. Equation [3] is often used in electrical engineering to describe the frequency characteristics of a low-pass filter and is only accurate when the voltage signal energy is equally distributed across the frequency bandwidth. This is not necessarily the case for the CS616 and ECH$_2$O Probe; therefore the frequencies calculated with Eq. [3] are only estimates. Additionally, the frequency estimates from Eq. [3] are for the EM signal before it passes from the sensor head into the medium; the signal frequency likely changes (decreases) in the medium. However, in NR-NC media the frequency change is likely small, and knowing an exact frequency at which the lower frequency sensing systems operate is not essential when deriving a response model due to the minimal dispersion observed in NR-NC media below a frequency of approximately 500 MHz (see Jones et al., this issue).

Responses in NR-NC media for each sensing system were produced by plotting network analyzer *e'* data, taken at the frequency determined (Table 3) for each sensing system, as a function of the sensing system outputs (i.e. travel time, period, voltage) as explained in Jones et al. (this issue). Response models (Table 3) for each sensing system were produced by fitting an

equation to the *e'* versus output data. Root mean squared error (RMSE) values were calculated to indicate how well the response models fit the data. The response models were used as *e'* prediction equations for all subsequent tests. The same response model is used for the two TDRs and Acclima TDT, and is derived from Eq. [1] omitting the factor of 2 and setting L_e = 0.15 m. It should be noted that the travel times for the Acclima TDT are divided by a factor of 4 to account for the longer probe length (0.60 m). The response models for the lower frequency sensing systems are empirical equations fit to the data using TableCurve (Jandel Scientific, San Rafael, CA).

The outputs of the sensing systems (excluding the CS616 and ECH_2O Probe; whose manufacturers do not provide information for calculating permittivity from sensor output) from the NR-NC media test were converted to *e'* values using Eq. [1] for the two TDRs and Acclima TDT, custom software for the Hydra Probe and Eq. [2] for the Theta Probe. The outputs from the R-NC media, NR-C media and temperature varying NR-NC media tests were input into the derived response models in order to produce a predicted sensor *e'* value (for the Hydra Probe the *e'* calculated by the custom software was used). The measurement accuracy of each sensing system under the different test conditions is inferred by calculating a residual value for each measurement in each test. The residual value is the difference between the reference and *e'* predicted by the sensing system being considered, and from these residual values, RMSE values are computed (Eq. [15] in Jones et al., this issue). For the NR-NC media (including the temperature variation test) and R-NC media, the Cole-Cole models fit to the network analyzer

measurements (Jones et al., this issue) serve as the reference. For NR-C media the *e'* value predicted by the given sensing system when medium s_b = 0.0 dS m^{-1} serves as the reference.

Sensor Measurement Weighting and Sampling Volume

The approximate sampling volume of each probe was estimated according to the method presented in Jones et al. (this issue). Briefly, this method employs the use of a computer program, the Arbitrary Transmission Line Calculator (ATLC) (Kirkby, 1996; 2003), which numerically calculates EM energy density distributions surrounding a specific transmission line geometry; and a Matlab® function (Humphries, 2004), which calculates the cross-sectional area within a specified minimum EM energy density contour. For our calculations we used a 10% EM energy density contour, thus the cross-sectional area contains all the values of EM energy density that are > 10% of the maximum value. The sampling volume is calculated by multiplying the cross-sectional area by the physical length of the probe. The coefficient of variation (CV) within the cross-sectional area is calculated by dividing the standard deviation of the EM energy density by the mean. The CV indicates the uniformity of the EM energy density surrounding the probe and is referred to as the measurement weighting.

RESULTS AND DISCUSSION

NR-NC Media

The maximum residuals and RMSE values for the NR-NC media (Table 4) indicate the accuracy of each sensing system in such media. The results indicate, that compared to the modeled e' values, the higher frequency broadband and lower frequency sensing systems both estimate e' values reasonably well (Figures 2 and 3). The network analyzer dielectric probe error is reported as ± 4 e' units within the frequency ranges or at the operating frequencies of the sensing systems considered. The Tektronix TDR, TDR100, Acclima TDT, Hydra Probe and Theta Probe all estimate e' within this range (Table 4), with the Theta Probe deviating the least and the Hydra Probe deviating the most from the modeled e' data. It should be noted that the CS616 and ECH_2O Probe were excluded in the NR-NC test (Table 4; Figure 3) because the manufacturers do not provide information for permittivity determination.

In relation to accurate EM signal property measurements, q_v prediction depends on a particular sensing system's ability to measure contrast as q_v changes. The response models (Figures 4a-4e) show that it is possible to detect e' differences over the entire range of permittivity covered in NR-NC media. However, there is much greater travel time (Figure 4a) and period contrast (Figure 4b) than there is output voltage contrast (Figures 4c-4e) above $e' \sim$ 40 ($e' \sim$ 25 for the ECH_2O Probe; Figure 4e). The Tektronix TDR, TDR100, Acclima TDT and CS616 show good contrast over the entire permittivity range, allowing the potential for accurate q_v prediction over the entire permittivity range found in soils ($e' \sim$ 2 to $e' \sim$ 60). The Hydra Probe, Theta Probe and ECH_2O Probe show minimal output voltage contrast in the permittivity range of $e' \sim$ 40 to $e' \sim$ 80. This implies that q_v prediction with these sensing systems in media with $e' >$ 40 will be difficult to perform with high accuracy. While it is likely that most soils have

ε' values within the 2 to 40 range, soils with high clay and/or organic matter contents and high porosity artificial growth media can have ε' values within the 40 to 80 range. In practice, media specific calibrations are often required due to the significant variation of dielectric properties among different porous media over the θ_v range from saturated to oven dry. The response models give good indication of the approximate ε' ranges and limits that the sensing systems considered should be used within.

R-NC and NR-C Media and Temperature Effects in NR-NC Media

Sensing system accuracy is also dependent on contrast caused by effects (i.e. relaxation, σ_b, temperature) other than θ_v changes. Relaxation (ε''_{rel}) has minimal effects on the high frequency broadband sensing system ε' estimates (Table 3), with errors increasing slightly as ε''_{rel} increases (Figure 5). However, the f_{max} decreases from the reported values (Table 3) to approximately 500 MHz for the two TDRs and 200 MHz for the Acclima TDT, owing to filtering of the higher frequency signal components brought about by energy dissipation during relaxation (Robinson et al., 2003b). In contrast, ε''_{rel} has greater effects on the Hydra Probe and Theta Probe (Table 4), causing both over-prediction and under-prediction of ε' values as ε''_{rel} increases (Figure 6). It should be noted that the CS616 and ECH_2O Probe were excluded in the R-NC test (Table 4; Figure 6) because their measurement frequencies in R-NC media cannot be estimated from Eq. [3] or network analyzer data because manufacturers do not provide information for permittivity determination.

Electrical conductivity (σ_b) affects the higher frequency broadband sensing systems to a greater extent than ε''_{rel} (Table 4), with ε' being under-predicted by the Tektronix TDR and over-predicted by the TDR100 and Acclima TDT as σ_b increases (Figures 7 and 8). The effects of σ_b are more pronounced in the lower permittivity media (ε_s = 40.0) (Figure 7) compared to the higher permittivity media (ε_s = 78.5) (Figure 8). The reason is inferred from the transmission line equation for a sinusoidal wave used as an analogy for transmission of a TDR signal (Eq. [6] in Jones et al., this issue). As ε' decreases, the ratio of the losses (i.e. ε''_{rel} and σ_{dc}, where $\sigma_{dc} = \sigma_b$ and is the dc frequency electrical conductivity) to ε' increases, thus modifying estimated permittivity to a greater extent. This phenomenon is demonstrated in Figure 5 in Robinson et al. (2003b).

The lower frequency sensors are much more sensitive to σ_b than ε''_{rel} (Table 4), except for the Hydra Probe, which shows similar sensitivities to σ_b and ε''_{rel}. Excluding the Hydra Probe, the lower frequency sensors are much more sensitive to σ_b than the higher frequency broadband sensors (Table 4). Increasing σ_b causes ε' over-prediction with the CS616 and ECH$_2$O Probe and ε' under-prediction with the Hydra Probe and Theta Probe in the lower permittivity (ε_s = 40.0) media (Figures 9 and 10; note the scale differences between these two figures and between Figs. 7 and 8). As stated above, the Hydra Probe estimates σ_b from the output voltage values and likely corrects ε' based on σ_b estimates, yielding accuracies similar to the higher frequency broadband sensing systems in NR-C media. In the higher permittivity (ε_s = 78.5) NR-C media the CS616 over-predicts ε' (graphical data not shown). It should be noted that NR-C

media data for the Hydra, Theta and ECH$_2$O Probes in the higher permittivity media are not shown because e_s = 78.5 is beyond the measurement range of these sensors (see Figures 4c-4e).

Temperature (T) affects e' predictions of the higher frequency broadband sensing systems to about the same magnitude as s_b (Table 4). Temperature < 35 °C causes e' over-prediction and T > 35 °C generally causes e' under-prediction in the lower permittivity (e_s = 40.0) media (Figure 11). The trend is reversed in the higher permittivity (e_s = 78.5) media; T < 25 °C causes e' under-prediction and T > 25 °C causes e' over-prediction (Figure 12). The observed trend reversal may be due in part to the relative temperature independence of the NR-NC media (e_s = 40.0) between approximately 1 and 2 GHz, caused by a temperature dependent shift in relaxation. For the lower frequency sensing systems, the temperature effects in the lower permittivity media are similar to those observed for the higher frequency broadband sensing systems (Table 4). Temperature < 25 °C generally causes e' over-prediction and T > 25 °C generally causes e' under-prediction, except for the CS616 where over-prediction was observed across the entire range (Figure 13). In the higher permittivity media, T effects cause under-prediction of e' at T < 25 °C and slight over-prediction at T > 25 °C for the CS616 (graphical data not shown). Why the higher frequency broadband sensing systems and the CS616 e' predictions do not fall near the reference at 25 °C in the lower permittivity media is unknown (Figures 11 and 13). The T range for the measurements in NR-NC media used to derive the response models is near 25 °C (Table 2), and thus e' predictions in the temperature varying NR-NC media test should be near the reference at 25 °C. It should be noted that data for T variation

in NR-NC media for the Hydra, Theta and ECH$_2$O Probes in the higher permittivity media are not shown for the same reason given above for the higher permittivity NR-C media.

The observed differences between the Tektronix TDR and TDR100 *e'* predictions (Table 4) are likely software related. The waveforms measured by the two TDR systems are nearly identical, thus the maximum residuals and RMSE values for the Tektronix TDR (Table 4) indicate that WinTDR software is superior to PCTDR software in interpreting measured waveforms. It is possible to interpret waveforms measured with each TDR sensing system with the same software (TACQ; Evett, 2000a; 2000b), but we considered software developed for use with certain systems (i.e. WinTDR for Tektronix TDRs and PCTDR for TDR100) as part of the sensing system.

Sampling Volume and Measurement Weighting

The Acclima TDT probe has a much larger estimated sampling volume than the other probes, while the ECH$_2$O Probe has the smallest estimated sampling volume (Table 5). The coefficient of variation of the EM energy density (CV $E\rho$ in Table 5) is the measurement weighting of each probe. The lower the CV $E\rho$ value, the more uniform the EM energy, which should yield a more uniformly weighted measurement. In contrast, a higher CV $E\rho$ value indicates more EM energy concentrated near the probe rods (i.e. 'skin' effect) and a measurement more heavily weighted to the media immediately surrounding the rods. The Acclima TDT shows the most uniform energy density while the Theta Probe shows the least uniform. The probe used with the two TDRs, the Hydra Probe and the CS616 all have similar

uniformity. The CV Eρ value reported for the ECH$_2$O Probe does not account for the plastic material surrounding the probe and is likely higher than what is reported. Those probes that display increased measurement weighting near the probe rods (high CV Eρ) increase the possibility for measurement error because soil near the rod surfaces is subject to greater disturbance during insertion, or non-uniform packing around the rods can occur if the medium is excavated in order to embed the probe.

CONCLUSIONS

A standard methodology for characterizing and comparing transmission line-type electromagnetic (EM) sensors designed for estimating soil volumetric water content (q_v) was proposed by Jones et al. (this issue). We demonstrated and tested this methodology by comparing seven sensing systems according to their measurement capabilities in media simulating conditions often observed in soils. The conditions included accuracy and range testing in non-relaxing and non-conducting (NR-NC) media simulating non-saline, sandy soils; and the effects of dielectric relaxation in relaxing and non-conducting (R-NC) media simulating low conductivity, clayey soils and electrical conductivity in non-relaxing and conducting (NR-C) media simulating saline, sandy soils. The effects of temperature varying conditions in NR-NC media were also tested. Attempts were made to produce relaxing and conducting (R-C) media simulating high conductivity, clayey soils in which the combined effects that these two phenomena have on measurements could be characterized. For reasons detailed in Jones et al. (this issue) we were unable to produce R-C media.

Under NR-NC test conditions (including temperature variation), the higher frequency broadband sensing systems (two time domain reflectometry (TDR) systems and one time domain transmissometry (TDT) system) and the lower frequency sensing systems (one transmission line oscillator, two impedance probes and one capacitance probe) showed similar measurement accuracy, with the TDRs, TDT and transmission line oscillator covering a larger real permittivity (e') range (1 to 80) than the others. The results from the R-NC, NR-C and temperature varying NR-NC test conditions indicate that for higher frequency systems, electrical conductivity (s_b) and varying temperature (T) have similar and greater effects on e' predictions than does relaxation (e''_{rel}). The results indicate that for lower frequency sensing systems s_b has the greatest effect on e' predictions, while varying T and e''_{rel} have similar effects. Compared to the higher frequency systems, the lower frequency systems were generally limited in the e' range (< 40) in which they can measure, and were generally more sensitive to s_b and e''_{rel}; especially s_b, under which condition all but one of the lower frequency sensing systems were extremely sensitive. This indicates that the frequency at which measurements are made is essential to accuracy in these media.

Calibration of EM sensors in order to estimate q_v is often a two-step process; first, relation of the measured EM signal property to e', and second, relation of e' to q_v. Conversely, some sensing systems employ a calibration from the measured signal property directly to q_v. With either two-step or direct calibration, the measured signal property is sensitive in some degree to e''_{rel}, s_b and T; leading to potential errors in q_v prediction if conditions vary from the calibration conditions. In addition, the permittivity determined is often sensor-dependent and

represents an apparent permittivity dependent on both ε' and imaginary permittivity (ε''). Based on the findings herein we suggest that more attention should be given to separation of ε' and ε'' because it is ε' that directly relates to θ_v. We also suggest that the measurement frequency should be increased because measurements are more sensitive to ε''_{rel} and σ_b at lower frequencies.

ACKNOWLEDGMENTS

The authors would like to extend special thanks to Bill Mace, Seth Humphries and Robert Heinse for their help in setting up the experiment and making the measurements and to Scott Anderson and Dr. Jim Ayers for technical assistance. The authors would also like to extend special thanks to the guest editor Dr. Steve Evett, Dr. Thijs Kelleners and two anonymous reviewers for carefully reviewing the manuscript and providing many helpful comments and insights. This project was supported by National Research Initiative Competitive Grant no. 2002-35107-12507 from the USDA Cooperative State Research, Education, and Extension Service.

REFERENCES

Blonquist Jr., J. M., S.B. Jones, and D.A. Robinson. A time domain transmission sensor with TDR performance characteristics. J. of Hydrol. (in review).

Bogart, T.F., J.S. Beasley, and G. Rico. 2004. Electronic Devices and Circuits. 6th ed. Prentice Hall, Columbus, OH, USA.

Campbell Scientific, Inc. 2002-2003. CS616 and CS625 Water Content Reflectometers Instruction Manual. Available at: http://www.campbellscientific.com/soilvol.html#cs616. (posted Apr. 2003; verified 21 Dec. 2004). Campbell Scientific, Inc., Logan, UT, USA.

Decagon Devices, Inc. 2002. ECH_2O Dielectric Aquameter User's Manual. Available at: http://www.ech2o.com/downloads.html (posted June 2002; verified 20 Dec. 2004). Decagon Devices, Inc., Pullman, WA, USA.

Delta-T Devices Ltd. 1999. Theta Probe Soil Moisture Sensor User Manual, pp. 47. Delta-T Devices, 128 Low Road, Burwell, Cambridge, CB5 0EJ, England.

Dirksen, C., and S. Dasberg. 1993. Improved calibration of time domain reflectometry soil water content measurements. Soil Sci. Soc. of Am. J. 57:660-667.

Evett, S.R. 2000a. The TACQ computer program for automatic time domain reflectometry measurements: I. Design and operating characteristics. Trans. of the ASAE 43:1939-1946.

Evett, S.R. 2000b. The TACQ computer program for automatic time domain reflectometry measurements: II. Waveform interpretation methods. Trans. of the ASAE 43:1947-1956.

Evett, S.R., B.B. Ruthardt, S.T. Kottkamp, T.A. Howell, A.D. Schneider, and J.A. Tolk. 2002. Accuracy and Precision of Soil Water Measurements by Neutron, Capacitance, and TDR Methods. p. 318-1 - 318-8. 17th World Conference of Soil Science Transactions, Bangkok, Thailand.

Fellner-Feldegg, H. 1969. The measurement of dielectrics in the time domain. J. of Phys. Chem. 73:613-623.

Friedman, S.P. 1998. A saturation degree-dependent composite spheres model for describing the effective dielectric constant of unsaturated porous media. Water Resour. Res. 34:2949-2961.

Gaskin, G.J., and J.D. Miller. 1996. Measurement of soil water content using a simplified impedance measuring technique. J. of Ag. Eng. Res. 63:153-159.

Hasted, J.B. 1973. Aqueous Dielectrics. Chapman and Hall, Cambridge, U. K.

Heimovaara, T.J. 1993. Design of triple-wire time domain reflectometry probes in practice and theory. Soil Sci. Soc. of Am. J. 57:1410-1417.

Heimovaara, T.J. 1994. Frequency domain analysis of time domain reflectometry waveforms 1. Measurement of the complex dielectric permittivity of soils. Water Resour. Res. 30:189-199.

Heimovaara, T.J., W. Bouten, and J.M. Verstraten. 1994. Frequency domain analysis of time domain reflectometry waveforms 2. A four-component complex dielectric mixing model for soils. Water Resour. Res. 30:201-209.

Hook, W.R., and N.J. Livingston. 1995. Errors in converting time domain reflectometry measurements of propagation velocity to estimates of soil water content. Soil Sci. Soc. of Am. J. 59:35-41.

Humphries, S.D. 2004. Software program for normalizing and extracting numerical data from ATLC [Online] http//:soilphysics.usu.edu/downloads/ATLCMatlabCode.html (verified 21 Dec. 2004).

Jacobsen, O.H., and P. Schjonning. 1993. A laboratory calibration of time domain reflectometry for soil water measurement including effects of bulk density and texture. J. of Hydrol. 151:147-158.

Jones, S.B., and D. Or. 2002. Surface area, geometrical and configurational effects on permittivity of porous media. J. of Non-Crys. Sol. 305:247-254.

Jones, S.B., and D. Or. 2003. Modeled effects on permittivity measurements of water content in high surface area porous media. Physica B 338:284-290.

Kirkby, D. 1996. Finding the characteristics of arbitrary transmission lines. Amateur Radio J. QEX:3-10.

Kirkby, D. 2003. Arbitrary Transmission Line Calculator (ATLC) Software [Online] http://atlc.sourceforge.net/ (verified 21 Dec. 2004).

Leib, B.G., J.D. Jabro, and G.R. Matthews. 2003. Field evaluation and performance comparison of soil moisture sensors. Soil Sci. 168:396-408.

Malicki, M.A., R. Plagge, and C.H. Roth. 1996. Improving the calibration of dielectric TDR soil moisture determination taking into account the solid soil. Euro. J. of Soil Sci. 47:357-366.

McMichael, B., and R.J. Lascano. 2003. Laboratory evaluation of a commercial dielectric soil water sensor. Vadose Zone J. 2:650-654.

Or, D., S.B. Jones, J.R. VanShaar, and J.M. Wraith. 2003. WinTDR 6.0 Users Guide (Windows-based TDR program for soil water content and electrical conductivity measurement). Available at: http://129.123.13.101/soilphysics/wintdr/documentation.htm (posted Fall 2003; verified 21 Dec. 2004). Utah Agric. Exp. Stn. Res., Logan, UT, USA.

Ponizovsky, A.A., S.M. Chudinova, and Y.A. Pachepsky. 1999. Performance of TDR calibration models as affected by soil texture. J. of Hydrol. 218:35-43.

Robinson, D.A., M. Schaap, S.B. Jones, S.P. Friedman, and C.M.K. Gardner. 2003a. Considerations for improving the accuracy of permittivity measurement using time domain

reflectometry: Air-water calibration, effects of cable length. Soil Sci. Soc. of Am. J. 67:62-70.

Robinson, D.A., S.B. Jones, J.M. Wraith, D. Or, and S.P. Friedman. 2003b. A review of advances in dielectric and electrical conductivity measurement in soils using time domain reflectometry. Vadose Zone J. 2:444-475.

Roth, K., R. Schulin, H. Fluhler, and W. Attinger. 1990. Calibration of time domain reflectometry for water content measurement using composite dielectric approach. Water Resour. Res. 26:2267-2273.

Seyfried, M.S., and M.D. Murdock. 2001. Response of a new soil sensor to variable soil, water content, and temperature. Soil Sci. Soc. of Am. J. 65:28-34.

Seyfried, M.S., and M.D. Murdock. 2004. Measurement of soil water content with a 50-MHz soil dielectric sensor. Soil Sci. Soc. of Am. J. 68:394-403.

Stevens Vitel, Inc. 1994. Hydra Soil Moisture Probe User's Manual. Manual and custom software HYDRA.exe, HYD_LOG.exe and HYD_FILE.exe available at http://www.stevenswater.com/soil_moisture_sensors/index.aspx (posted 8 July 1998; verified 21 Dec. 2004). Stevens Vitel, Inc., Beaverton, OR, USA.

Topp, G.C., J.L. Davis, and A.P. Annan. 1980. Electromagnetic determination of soil water content: measurements in coaxial transmission lines. Water Resour. Res. 16:574-582.

Topp, G.C., J.L. Davis, and A.P. Annan. 1982. Electromagnetic determination of soil water content using TDR: I. Applications to wetting fronts and steep gradients. Soil Sci. Soc. of Am. J. 46:672-678.

Walker, J.P., G.R. Willgoose, and J.D. Kalma. 2004. In situ measurements of soil moisture: A comparison of techniques. J. of Hydrol. 293:85-99.

Whalley, W.R. 1993. Considerations on the use of time domain reflectometry (TDR) for measuring soil water content. J. of Soil Sci. 44:1-9.

Table 1. Principle of operation, required equipment and cost breakdown for the sensing systems considered in the study.

	Tektronix TDR	TDR100	Acclima TDT	CS616	Hydra Probe	Theta Probe	ECH_2O Probe
Principle of Operation	TDR†	TDR†	TDT†	TLO†	Impedance	Impedance	Capacitance
Equipment Required	Analysis software	Data logger, Analysis software	Custom controller, Custom software	Data logger	Data logger, Custom software	Data logger	Data logger
Cost for Single Sensor:							
Sensor cost	$11,765	$3,720	$349	$175	$324	$460	$100
Data logger‡ or controller	--	$1,250	$2,580	$750	$750	$750	$750
Total cost	$11,765	$4,970	$2,929	$925	$1074	$1210	$850
Cost for Eight Sensors:							
+ 7 sensors	$490	$490	$2,443	$1,225	$2,268	$3,220	$700
Multiplexer	$450	$450	--	$545	$545	$545	$545
Total cost	$12,705	$5,910	$5,372	$2,695	$3,887	$4,975	$2,095

†Time domain reflectometry (TDR), time domain transmissometry (TDT) and transmission line oscillation (TLO).

‡Data logger price listed is for the Campbell Scientific CR10X for TDR100 and CR510 for the CS616, Hydra Probe, Theta Probe and ECH_2O Probe.

Table 2. Medium components, properties and temperature (T) ranges for the different test conditions.

NR-NC	R-NC	NR-C	Temperature effects in NR-NC
2-iso/di-water solutions: e_s = 12.7 to 78.5† s_b = 0.0 dS/m‡ T = 23.9 to 24.7 °C	**Glycerol:** e_s = 46.5 s_b = 0.0 dS/m **Brasso®§:** e_s = 28.0 s_b = 0.0 dS/m **1-propanol:** e_s = 22.8 s_b = 0.0 dS/m T = 23.8 to 24.3 °C	**2-iso/di-water solution:** e_s = 40.0 s_b = 0.0 to 2.0 dS/m T = 24.5 to 24.7 °C **di-water:** e_s = 78.5 s_b = 0.0 to 2.0 dS/m T = 24.4 to 24.6 °C	**2-iso/di-water solution:** e_s = 38.5 to 41.3 s_b = 0.0 dS/m T = 5.38 to 39.5 °C **di-water:** e_s = 73.4 to 86.1 s_b = 0.0 dS/m T = 5.05 to 40.0 °C

†e_s denotes the static real permittivity component determined from the Cole-Cole modeled network analyzer data.

‡s_b denotes the dc electrical conductivity measured with a standard electrical conductivity meter.

§Brasso® was used as a reference in the sensor comparison herein because it is readily available and is characterized by significant relaxation in the frequency range of the sensing sytems tested, however, Jones et al. (this issue) do not recommend it as a standard reference R-NC medium because it is a proprietary product.

Table 3. Response models used to predict real permittivity (*e'*) values from output travel time, period or voltage for each sensing system.

Sensor	Frequency†	Response Model‡	RMSE
ECH_2O Probe	50 MHz	$\frac{1}{e'} = -0.0501 + \frac{0.0607}{V^2}$	0.0573
CS616	200 MHz	$\sqrt{e'} = -4.61 + 0.550\ln(p) + \sqrt{p}$	0.0414
Hydra Probe	50 MHz	NA§	NA§
Theta probe (e_s = 1 to 43)	100 MHz	$\frac{1}{e'} = -0.105 + \frac{0.134}{\sqrt{V}}$	0.0664
Theta Probe (e_s = 43 to 80)	100 MHz	$\frac{1}{e'} = 0.0279 - 0.767(\ln V)^2$	0.0947
Acclima Digital TDT	1.23 GHz	$e' = \left(\frac{ct}{L_e}\right)^2$	0.0489
TDR100	1.45 GHz	$e' = \left(\frac{ct}{L_e}\right)^2$	0.0415
Tektronix TDR	1.64 GHz	$e' = \left(\frac{ct}{L_e}\right)^2$	0.0375

†No published frequencies are available for the ECH_2O Probe and CS616, those listed were estimated with Eq. [3] (~ maximum passable frequency, f_{max}) using rise times of 2 ns (Campbell Scientific, personal communication) and 8 ns (Decagon Devices, personal communication), respectively; frequencies for the Hydra Probe and Theta Probe are the published sensing system frequencies (Seyfried and Murdock, 2004; Gaskin and Miller, 1996; respectively) and frequencies for the Acclima Digital TDT, TDR100 (connected to a 0.15-m three-rod probe) and Tektronix TDR (connected to a 0.15-m three-rod probe) are average f_{max} values determined in NR-NC media ranging from static real permittivity (e_s) = 12.7 to 62.8 (Blonquist et al., in review).

‡Symbols are as follows: *e'* = real permittivity, *V* = volts, *p* = period, *t* = travel time, *c* = speed of light in free space, L_e = probe electrical length.

§A response model for the Hydra Probe was not derived because manufacturer information concerning how V_1, V_2 and V_3 are used to compute permittivity was not available. Hydra software (Hydra.exe) was used to determine *e'*.

Table 4. Maximum residual (reference – prediction) of real permittivity (*e'*) and root mean squared error (RMSE) values for each sensing system.

	Tektronix TDR	TDR100	Acclima Digital TDT	CS616	Hydra Probe	Theta Probe	ECH_2O Probe
NR-NC†							
Max Residual of *e'*	+ 1.95	+ 2.94	+ 2.76	NA‡	- 3.94	- 1.92	NA‡
RMSE	0.805	1.72	0.947	NA‡	1.07	0.545	NA‡
R-NC†							
Max Residual of *e'*	- 0.206	+ 0.279	- 0.511	NA§	- 2.70	- 3.28	NA§
RMSE	0.164	0.222	0.388	NA§	1.60	2.50	NA§
NR-C†							
e_s = 40.0							
Max Residual of *e'*	- 1.86	+ 2.69	+ 1.70	+ 23.2	- 2.24	- 9.65	+ 111
RMSE	1.07	1.42	1.01	12.4	1.98	6.51	65.5
e_s = 78.5							
Max Residual of *e'*	- 2.00	+ 1.06	+ 0.872	- 9.64#	NA¶	NA¶	NA¶
RMSE	1.16	0.701	0.604	6.84#	NA¶	NA¶	NA¶
Temperature effects in NR-NC†							
e_s = 38.5 to 41.3							
Max Residual of *e'*	+ 3.38	+ 4.89	+ 3.34	+ 5.98	- 2.98	- 1.28	+ 2.78
RMSE	2.11	2.49	2.16	4.07	1.78	0.657	1.78
e_s = 73.4 to 86.1							
Max Residual of *e'*	- 0.975	+ 1.72	- 2.41	- 6.59#	NA¶	NA¶	NA¶
RMSE	0.497	0.925	1.26	3.28#	NA¶	NA¶	NA¶

†Properties of each medium are listed in Table 1, e_s denotes static real permittivity.

‡Data unavailable for CS616 and ECH_2O Probe because the manufacturers do not provide information for direct permittivity determination.

§Data unavailable for CS616 and ECH_2O Probe due to variability of sensor frequency in R-NC media and inability to estimate frequency owing to lack of information for direct permittivity determination.

¶Data not reported because medium permittivity is beyond the measurement range of these sensors (measurement ranges extend to $e_s \sim 40$; see Figure 4).

#Graphical data are not shown in a figure.

Table 5. Sampling volume and measurement weighting within a 10% electromagnetic energy density contour for each sensor.

	Tektronix TDR and TDR100‡	Acclima Digital TDT	CS616	Hydra Probe	Theta Probe	ECH_2O Probe§
Sampling Volume [cm^3]	24.5	133	39.6	9.47	7.62	1.99
CV Eρ†	0.689	0.600	0.700	0.668	0.736	0.709

†Denotes the coefficient of variation (CV) of the electromagnetic energy density (Eρ) surrounding the probe.

‡The same probe was used with the Tektronix TDR and CSI TDR100.

§Calculation of CV Eρ does not account for plastic surrounding probe.

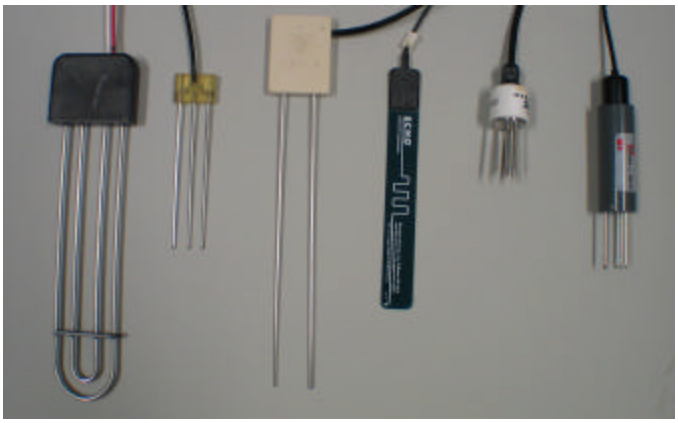

Figure 1: Probes of the sensing systems considered in the study are from left to right: Acclima Digital TDT Sensor, 3-rod TDR probe used with Tektronix TDR and TDR100 (0.15-m long 3.20 mm diameter rods, 12.0-mm rod spacing), CS616, ECH$_2$O Probe, Hydra Probe and Theta Probe.

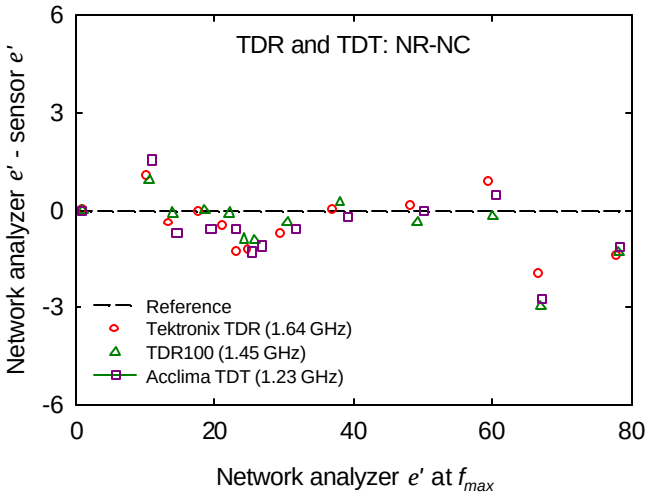

Figure 2: Deviation of higher frequency broadband sensing system *e'* predictions from the modeled network analyzer *e'* measurements (reference) in NR-NC media. The frequencies from which the reference *e'* measurements were taken are in parentheses and are maximum passable frequencies (f_{max}).

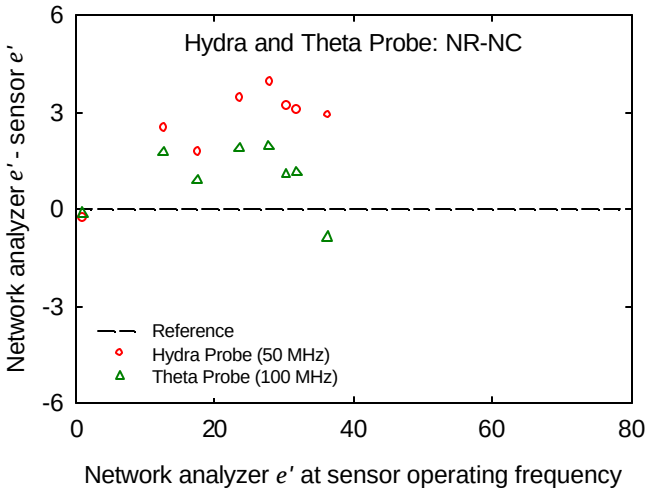

Figure 3: Deviation of the lower frequency sensing system (excluding CS616 and ECH_2O Probe) *e'* predictions from the modeled network analyzer *e'* measurements (reference) in NR-NC media. The frequencies from which the reference *e'* measurements were taken are in parentheses and are reported sensor frequencies. The x-axis ranges from 0 to 80 to indicate the measurement range compared to the higher frequency broadband sensing systems (Figure 2). Note: the CS616 and ECH_2O Probe are excluded because the manufacturers do not provide information for permittivity determination.

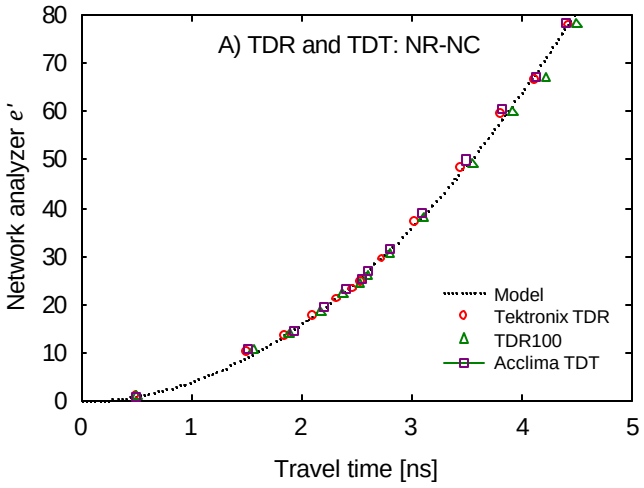
A) TDR and TDT: NR-NC
Network analyzer e'
Travel time [ns]
Model
Tektronix TDR
TDR100
Acclima TDT

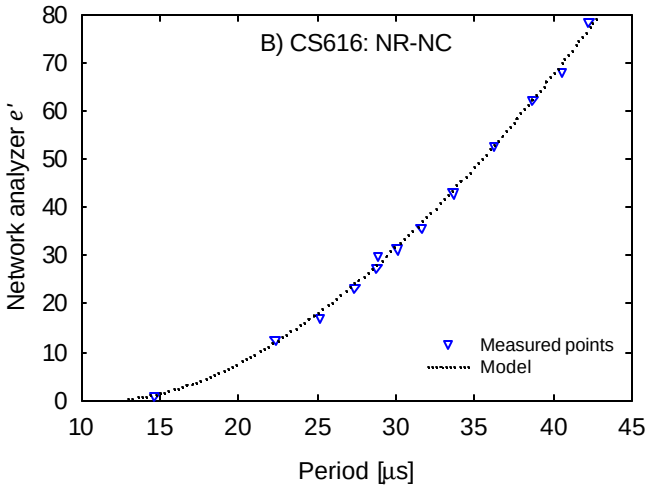
B) CS616: NR-NC
Network analyzer e'
Period [µs]
Measured points
Model

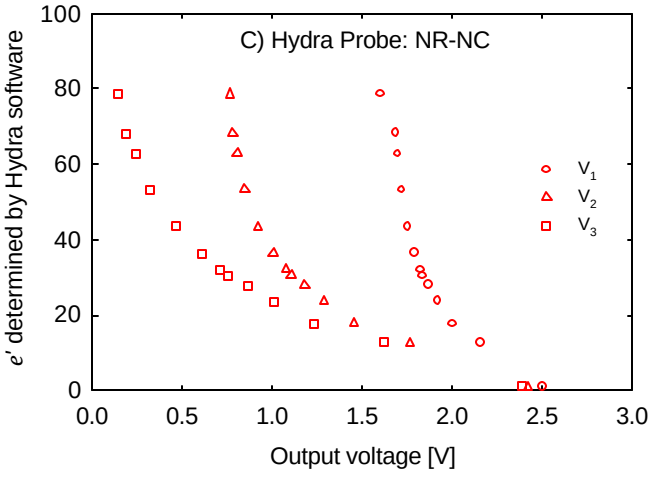
C) Hydra Probe: NR-NC
e' determined by Hydra software
Output voltage [V]
V1
V2
V3

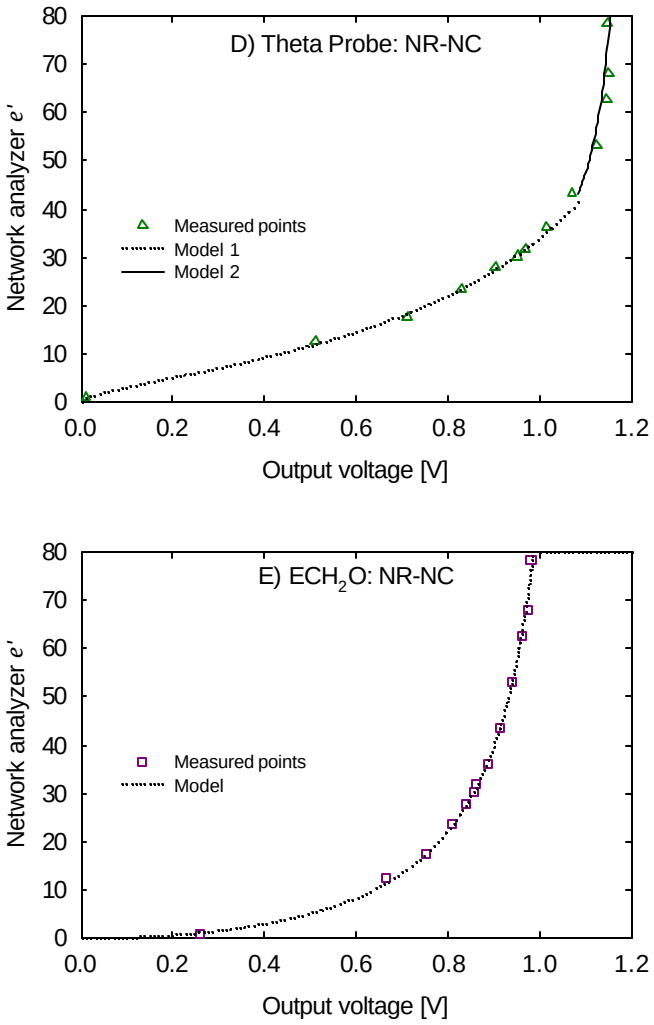

Figure 4: Response models fit to the NR-NC media data for the a) higher frequency broadband sensing systems (model is Eq. [1] fit to the data using an electrical length (L_e) of 0.15-m, and where the travel times measured with the Acclima TDT are divided by a factor of four to account for 0.60-m waveguide length), b) CS616, c) Hydra Probe (response model was not derived for the Hydra Probe because it uses three output voltage values to derive permittivity and the details concerning how this is accomplished were not available from the manufacturer), d) Theta Probe and e) ECH_2O Probe. The models for the CS616, Theta Probe and ECH_2O Probe are empirical equations fit to the data with TableCurve (Jandel Scientific, San Rafael, CA).

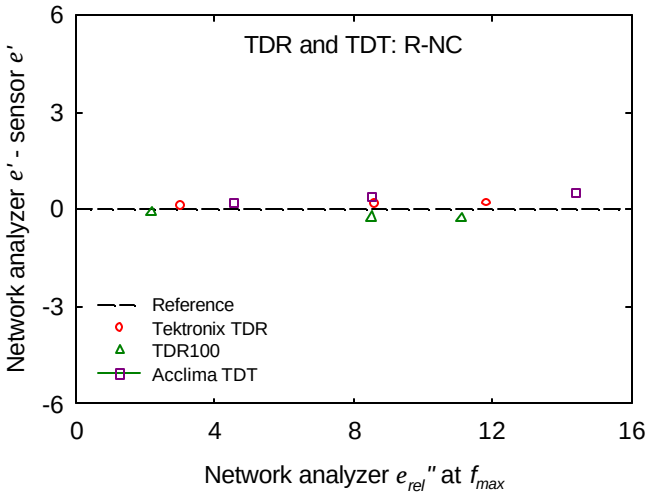

Figure 5: Deviation of higher frequency broadband sensing system e' predictions (from response model) from modeled network analyzer e' measurements (reference) in R-NC (Table 2) media as relaxation (e_{rel}'') increases. The frequencies from which the reference network analyzer e' measurements were taken are the individual maximum passable frequencies (f_{max}) of the sensing systems in the three R-NC media samples (glycerol, Brasso® and 1-propanol). It should be noted that the f_{max} values in R-NC media are reduced by approximately 1 GHz compared to NR-NC media.

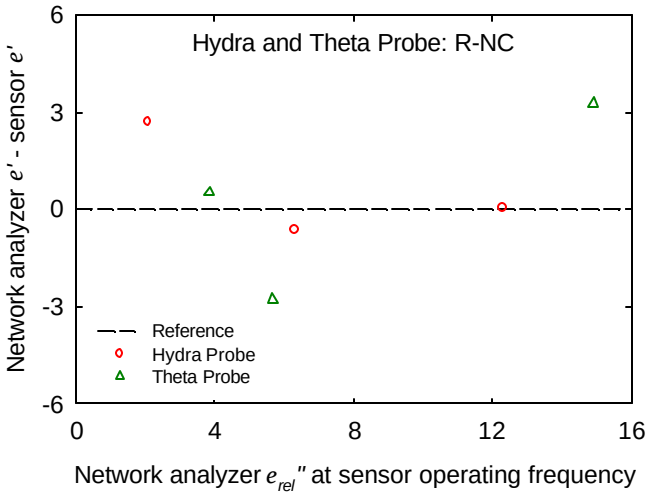

Figure 6: Deviation of lower frequency sensing system (excluding the CS616 and ECH_2O Probe) *e'* predictions (from software for Hydra Probe and response model for Theta Probe) from modeled network analyzer *e'* measurements (reference) in R-NC media (Table 2) as relaxation (e_{rel}") increases. Note: the CS616 and ECH_2O Probe are excluded because their measurement frequencies in R-NC media and cannot be estimated from Eq. [3], or inferred from network analyzer data (manufactures do not provide information for permittivity determination).

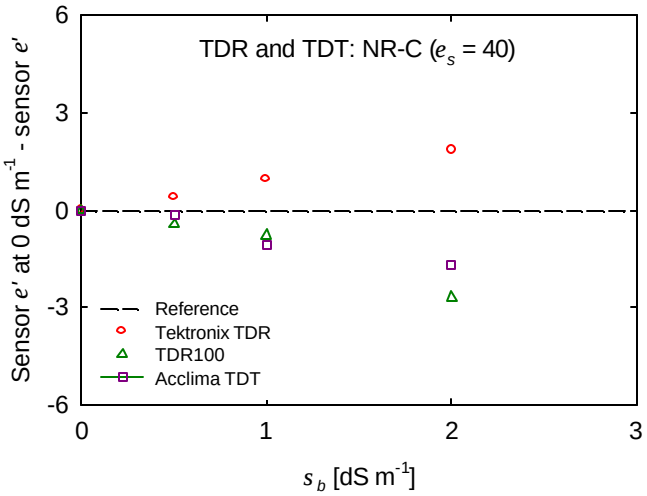

Figure 7: Deviation of higher frequency broadband sensing system *e'* predictions from the *e'* prediction where electrical conductivity (s_b) = 0.0 dS m^{-1} (reference) as NR-C sample s_b increases from 0.0 to 2.0 dS m^{-1}. The NR-C sample used here has a e_s = 40.0 (Table 2).

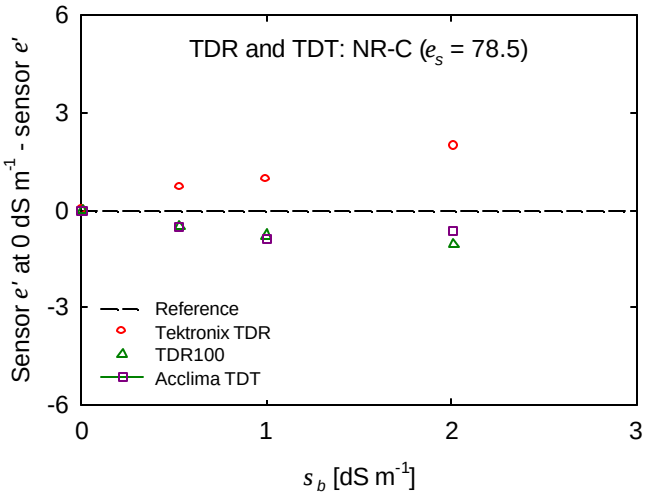

Figure 8: Deviation of higher frequency broadband sensing system e' predictions from the e' prediction where electrical conductivity (s_b) = 0.0 dS m^{-1} (reference) as NR-C sample s_b increases from 0.0 to 2.0 dS m^{-1}. The NR-C sample used here has a e_s = 78.5 (Table 2).

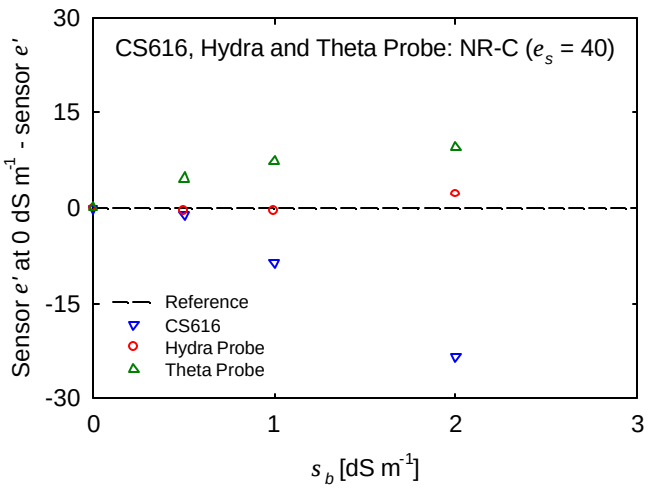

Figure 9: Deviation of lower frequency sensing system (excluding ECH$_2$O Probe; see Figure 11) e' predictions from the e' prediction where electrical conductivity (s_b) = 0.0 dS m^{-1} (reference) as NR-C sample s_b increases from 0.0 to 2.0 dS m^{-1}. The NR-C sample used here has a e_s = 40.0 (Table 2).

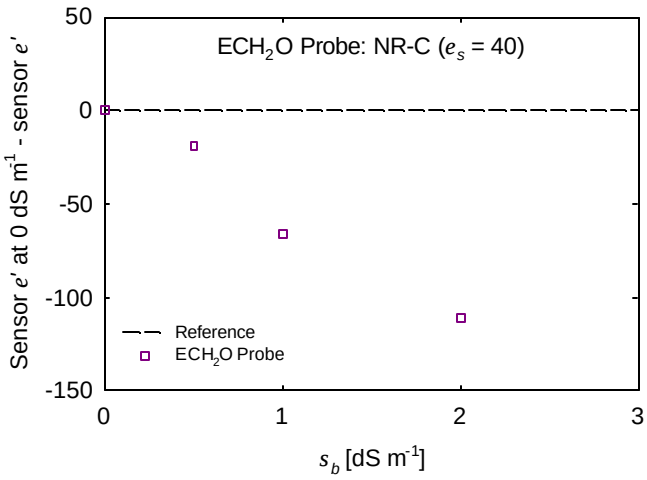

Figure 10: Deviation of ECH_2O Probe *e'* predictions from the *e'* prediction where electrical conductivity (s_b) = 0.0 dS m^{-1} (reference) as NR-C sample s_b increases from 0.0 to 2.0 dS m^{-1}. The NR-C sample used here has a e_s = 40.0 (Table 2).

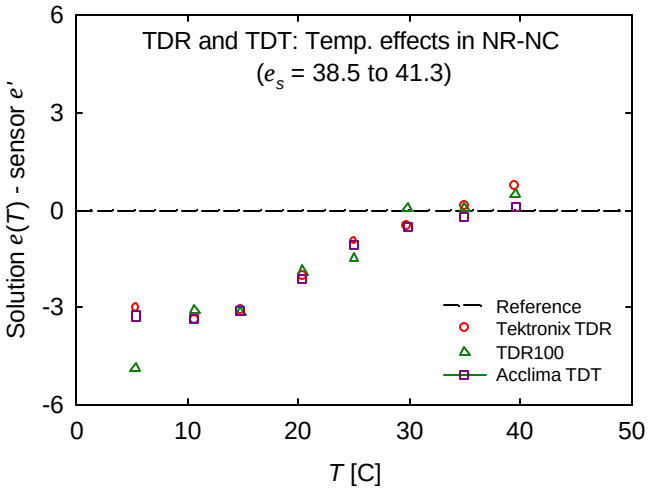

Figure 11: Deviation of higher frequency broadband sensing system *e'* predictions from modeled network analyzer *e'* measurements in NR-NC media with a temperature (*T*) range of 5.38 to 39.5 °C (Table 2). The NR-NC sample used here has a e_s = 38.5 to 41.3 (Table 2).

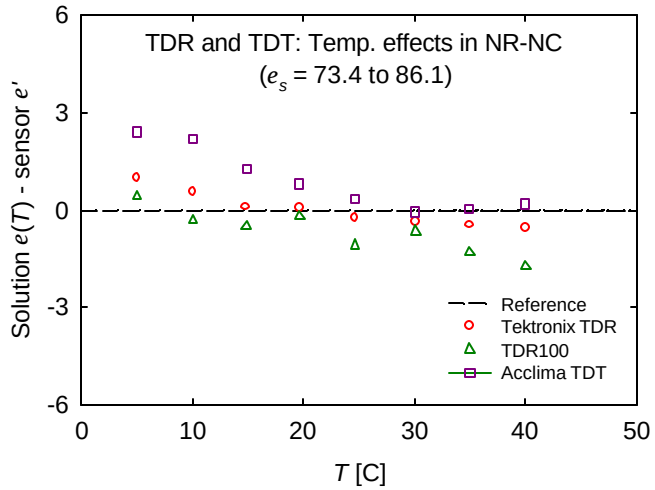

Figure 12: Deviation of higher frequency broadband sensing system *e'* predictions from modeled network analyzer *e'* measurements in NR-NC media with a temperature range of 5.05 to 40.0 °C (Table 2). The NR-NC sample used here has a e_s = 73.4 to 86.1 (Table 2).

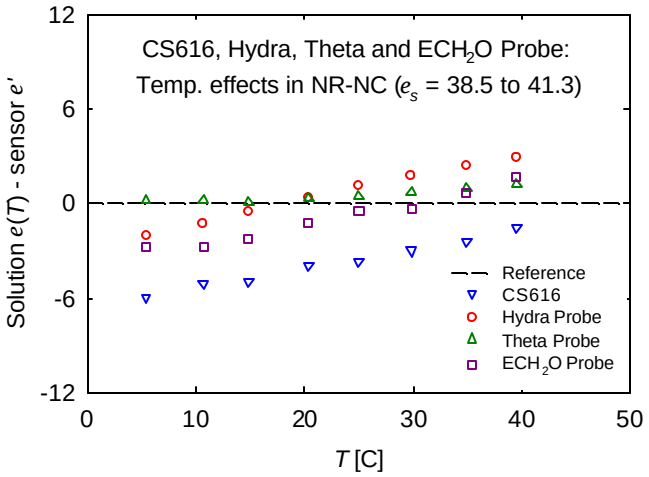

Figure 13: Deviation of lower frequency sensing system *e'* predictions from modeled network analyzer *e'* measurements in NR-NC media with a temperature (*T*) range of 5.38 to 39.5 °C (Table 2). The NR-NC sample used here has a e_s = 38.5 to 41.3 (Table 2).